

Imaging Molecular and Nanoscale Order in Conjugated Polymer Thin Films with Near-field Scanning Optical Microscopy

Julie A. Teetsov[‡] and David A. Vanden Bout*

Department of Chemistry and Biochemistry
Center for Nano- and Molecular Science and Technology
Texas Materials Institute, University of Texas
Austin, Texas 78712

Received January 17, 2001

There has been wide interest in the properties of conjugated polymer thin films since the first demonstrations of polymer light-emitting devices in the early 1990s.^{1,2} The complex structure of polymer films coupled with the tendency for these systems to have electronic interactions between polymer chains has led to controversy about the nature of the light-emitting species and carrier dynamics in films. Interpolymer species have been indicated to both decrease and increase the quantum yield for emission,^{3–9} as well as both increase and decrease the charge carrier mobility.^{10–12} These contradictions present the need for nanoscale characterization to obtain a clear picture of the molecular structure in these systems. This is particularly true in applications with ordered films such as polarized light-emitting devices^{13,14} or polymer lasers.¹⁵ Many conjugated polymer films have liquid crystalline (LC) properties that cause the chains to self-order in films¹⁶ and can be used to create highly ordered annealed films.¹⁷ It has generally been believed that the polymers adopt a nematic LC order within the annealed films. However, we report in this communication that annealed films of the conjugated polymer poly(9,9 dihexylfluorene) (PDHF), inset in Figure 1, display a more complex structure on the nanometer length scale. Near-field scanning optical microscopy^{18,19} is used to determine that the polymers pack into long ribbonlike structures whose long axis is perpendicular to the polymer backbone. Such structures affect the migration of excitations in these systems and demonstrate the need for careful nanoscale characterization of conjugated polymer films.

The effect of interpolymer interactions in PDHF films can be observed in their fluorescence spectra. The fluorescence spectra

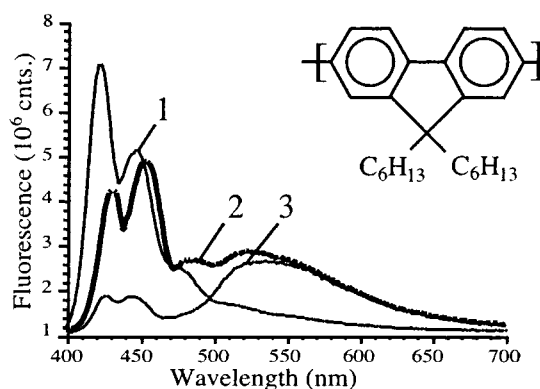


Figure 1. Fluorescence spectra of pristine (1), 2-h annealed (2), and 12-h annealed (3) PDHF films.

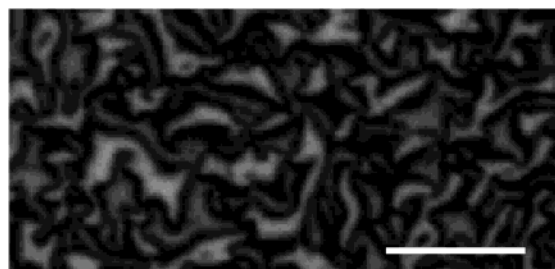


Figure 2. Polarized light micrograph of an annealed PDHF film view through crossed polarizers. Scale bar is 10 micrometers.

of 170 nm spin-coated films are shown in Figure 1 for a pristine “as-spun” film and films annealed for 2 and 12 h. Films were annealed by heating them just above their LC phase transition (250 °C) in a dry nitrogen atmosphere and holding them at this temperature for 2 or 12 h before rapidly cooling them. The increase in polymer order with annealing leads to a decrease in the fluorescence at 420 nm and a new band growing in around 550 nm. These changes are accompanied by two new long-lived fluorescent species at low energies.¹⁰ These species have been assumed to be due to increase in the overlap of π -electrons between polymer chains in the films due to partial alignment in the nematic phase. The LC order has been thought to be nematic on the basis of the high polydispersity of most conjugated polymer samples and images from conventional polarized light microscopy (PLM). Some previous X-ray diffraction studies have shown the order to be more complex.^{9,18} A PLM micrograph is shown in Figure 2 and displays the Schlieren texture indicative of nematic order.

Near-field scanning optical microscopy (NSOM) reveals a richer structure not seen in the far field experiments. NSOM is a scanning probe microscopy (SPM) technique that simultaneously collects nanoscale topographic and fluorescence images by scanning with a force feedback mechanism in the near-field with a sub-wavelength aperture fiber optic probe. There have only been a few NSOM or SPM studies of conjugated polymer films.^{17,21–22} The NSOM apparatus and PDHF used in these studies have been previously described.¹⁷ Figure 3 shows the topography of PDHF films annealed 2 and 12 h. The topography of the pristine films shows 50–150 nm clusters that form due to insolubility in the

[‡] Present address: General Electric Corporate Research and Development, Materials Characterization Laboratory, Bldg. K1-1C10, P.O. Box 8, Schenectady, NY 12301.

(1) Burroughes, J. H.; Bradley, D. D. C.; Marks, R. N.; Mackay, K.; Friend, R. H.; Burn, P. L.; Holmes, A. B. *Nature* **1990**, 347, 539–541.
(2) Gustafsson, G.; Cao, Y.; Treacy, G. M.; Klavetter, F.; Colaneri, N.; Heeger, A. J. *Nature* **1992**, 357, 477–479.
(3) Jenekhe, S. A.; Osaheni, J. A. *Science* **1994**, 265, 765–768.
(4) Jakubiak, R.; Collison, C. J.; Wai, C. W.; Rothberg, L. J. *J. Phys. Chem. B* **1999**, 103, 2394–2398.
(5) Shi, Y.; Liu, J.; Yang, Y. *J. Appl. Phys. Lett.* **2000**, 87, 4254–4263.
(6) Bliznyuk, V. N.; Carter, S. A.; Scott, J. C.; Klärner, G.; Miller, R. D.; Miller, D. C. *Macromolecules* **1999**, 32, 361–369.
(7) Conwell, E. *Trends Polym. Sci.* **1997**, 5, 218–222.
(8) Grell, M.; Bradley, D. D. C.; Long, X.; Chamberlain, T.; Inbasekaran, M.; Woo, E. P.; Soliman, M. *Acta Polym.* **1998**, 49, 439–444.
(9) Teetsov, J.; Fox, M. A. *J. Mater. Chem.* **1999**, 9, 2117–2122.
(10) Redecker, M.; Bradley, D. D. C. *Appl. Phys. Lett.* **1999**, 74, 1400.
(11) Tasch, S.; Niko, A.; Leising, G. *Appl. Phys. Lett.* **1996**, 68, 1090.
(12) Parker, I. D.; Cao, Y.; Yang, C. Y. *J. Appl. Phys.* **1999**, 85, 2441.
(13) Weder, C.; Sarwa, C.; Montali, A.; Bastiaansen, C.; Smith, P. *Science* **1998**, 279, 835–837.
(14) Miller, E. K.; Maskel, G. S.; Yang, C. Y.; Heeger, A. J. *Phys. Rev. B* **1999**, 60, 8028–8033.
(15) Hide, F.; Diaz-Garcia, M. A.; Heeger, A. J. *Acc. Chem. Res.* **1997**, 30, 430–436.
(16) Teetsov, J.; Vanden Bout, D. A. *J. Phys. Chem. B* **2000**, 140, 9378.
(17) Grell, M.; Bradley, D. D. C.; Inbasekaran, M.; Woo, E. P. *Adv. Mater.* **1997**, 9, 798–802.
(18) Dunn, R. C.; *Chem. Rev.* **1999**, 99, 2891–2927.
(19) Vanden Bout, D. A.; Kerimo, J.; Higgins, D. A.; Barbara, P. F. *Acc. Chem. Res.* **1997**, 30, 204–212.

(20) Blatchford, J. W.; Gustafson, T. L.; Epstein, A. J.; Vanden Bout, D. A.; Kerimo, J.; Higgins, D. A.; Barbara, P. F.; Fu, D.-K.; Swager, T. M.; MacDiarmid, A. G. *Phys. Rev. B* **1996**, 54, R3683–R3686.

(21) DeAro, J. A.; Weston, K. D.; Buratto, S. K.; Lemmer, U. *Chem. Phys. Lett.* **1997**, 277, 532–538.

(22) Nguyen, T.-Q.; Martini, I.; Liu, J.; Schwartz, B. J. *J. Phys. Chem. B* **2000**, 104, 237–255.

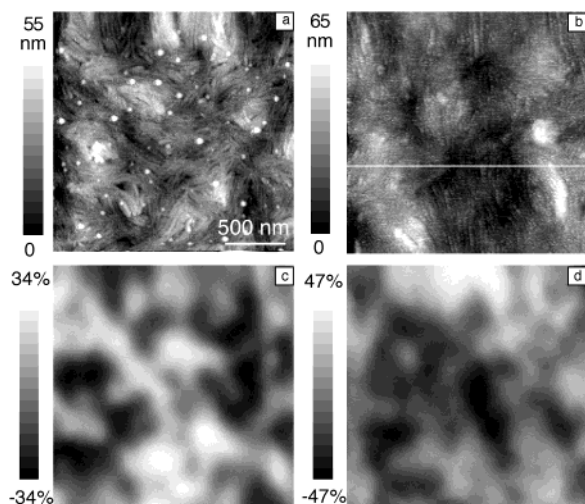


Figure 3. $2 \times 2 \mu\text{m}$ topography (a,b) and NSOM fluorescence anisotropy (c,d) of 2-h (a,c) and 12-h (b,d) annealed PDHF films.

spinning solution prior to spin-coating.¹⁷ Upon annealing, the clusters shrink, and the polymer begins to pack into ribbons that are 40–70 nm wide and 500 nm to $1 \mu\text{m}$ long; longer annealing times increase the length but not the width of these features. The degree of order within these structures can be quantified with the NSOM fluorescence image. Since the dipole of PDHF is along the backbone of the polymer, the polarization of the emission provides information about the molecular orientation. A measure of the molecular order can be made using two polarized fluorescence images collected at orthogonal polarizations. From these images an anisotropy (or linear dichroism) image is calculated from the difference in intensity in the two polarizations normalized to the total intensity¹⁷ (+100% = purely horizontal, –100% = purely vertical). The NSOM fluorescence anisotropy images are shown in Figure 3. The overall order in the image is assessed on the basis of the standard deviation of the distribution of anisotropy values from all of the pixels in the image. An average of these standard deviations for many samples gives anisotropy values of 12.5 and 23.6% for 2- and 12-h annealed PDHF films, respectively. The anisotropy is slightly different from the standard order parameter, S , used to quantify nematic liquid crystalline order, because the anisotropy reflects only the in-plane alignment along an arbitrary direction (horizontal in the image) rather than the three-dimensional alignment along the liquid crystal director. The maximum anisotropy in the 2- and 12-h sample are 34 and 47%, respectively. Assuming the director for the regions of maximum anisotropy are along the horizontal axis, the order parameter S is 0.51 and 0.60 in the 2- and 12-h samples, respectively. The maximum anisotropy value of 100% is not observed in any region because the ordered regions are not aligned throughout the depth of the film. Because the NSOM excitation is not completely absorbed in the top region of the film, domains below the first layer in the film that are not oriented in the same direction will wash out the net anisotropy. Modeling of the film as a grid of perfectly ordered 50 nm cubic domains that are randomly ordered throughout the film reproduces both the maximum and standard deviation anisotropy values.¹⁷

The polarization also reveals the structure of the polymer within the lamellae. The intensity of fluorescence is greatest when collected perpendicular to the lamellae's long axis as shown in Figure 3 and Figure 4. Since the fluorescence is polarized along the polymer backbone, this shows that the lamellae are composed of polymers stacked orthogonal to the lamellae's long axis. A similar structure has been proposed by Rabe et al. for nanoribbons of PPE characterized using AFM.²³ The Schlieren texture in the

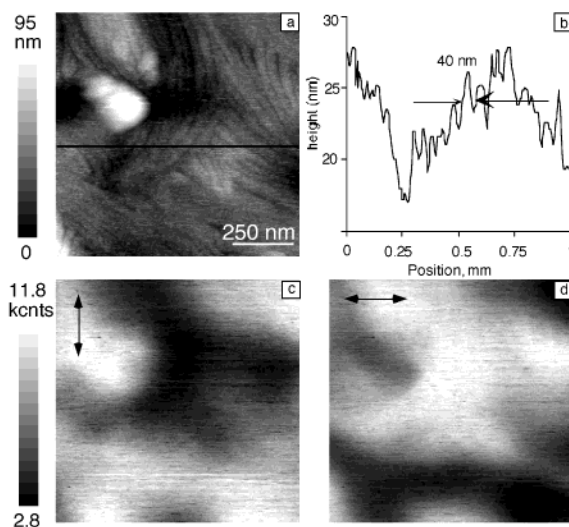


Figure 4. $1 \times 1 \mu\text{m}$ images of 12-h annealed PDHF. (a) Topography, (b) line scan across topography, (c) horizontal, and (d) vertical polarized NSOM fluorescence.

PLM is the result of the lamellae orienting with directors around disclination defects rather than the polymers themselves. The lamellae width are all around 40 nm in the topography measurements. Due to the high polydispersity it is unlikely that the ribbons are composed of single fully extended chains. More likely they are made up of a few chains. The high anisotropy value and NSOM simulations indicated that structure must maintain its order for around 50 nm into the depth of the film. Such a structure will have very different carrier dynamics compared to either a completely isotropic or simple nematic film. As the film is annealed from 2 to 12 h, the intrapolymer emission is almost completely quenched. The strong reduction in intrapolymer emission indicates that the initial excitations are able to migrate to low-energy interpolymer sites more readily in the fully developed lamellar structure. The fact that the structures increase in length rather than width as the film is annealed suggests that there is a larger mobility along the lamella than there is perpendicular to this secondary structure.

With an understanding of the molecular structure in the annealed films, NSOM can be used to further study the inter- and intrapolymer emitting species by imaging with two wavelengths. Simultaneous images at 400 and 660 nm show identical contrast indicating the inter- and intrapolymer species are dispersed evenly in the films even in the highly ordered lamellae structures. Polarization studies at these wavelengths also indicate that the interpolymer species have the same polarization as the intrapolymer species.

In conclusion, we have used the correlated topography and optical information to reveal a complex molecular structure in annealed PDHF films. The results indicate annealed and aligned conjugated polymer systems have a richer morphology than previously believed, and this structure has a strong impact on the emission and carrier dynamics in the systems. The highly ordered ribbonlike features in the 12-h annealed PDHF films create both a high number of interpolymer sites as well as increase the mobility of excitations in the film.

Acknowledgment. We gratefully acknowledge Dr. E. P. Woo and Dr. M. Inbasekaran at Dow Chemical for the polymer samples used in this study. We also thank Dr. Stefan Kaemmer at ThermoMicroscopes. This research is supported by the NSF and the Welch Foundation. D.V.B. thanks the Dreyfus Foundation for a New Faculty Award and is a Research Corporation Cottrell Scholar.

(23) Samori, P.; Francke, V.; Mullen, K.; Rabe, J. P. *Chem. Eur. J.* **1999**, *5*, 2312–2317.